AD-A038 141 SYRACUSE UNIV N Y DEPT OF ELECTRICAL AND COMPUTER E--ETC F/G 9/5

APPLICATION OF MOM/GTD TECHNIQUES TO SHIPBOARD ANTENNAS.(U)

JAN 77 J PERINI, C CHEN F30602-75-C-0121

UNCLASSIFIED RADC-TR-77-43 NL

1 OF 1

AD A038141

END

DATE FILMED

5-77

RADC-TR-77-43
Technical Report
January 1977

APPLICATION OF MOM/GTD TECHNIQUES TO SHIPBOARD ANTENNAS

Syracuse University

ROME AIR DEVELOPMENT CENTER
AIR FORCE SYSTEMS COMMAND
GRIFFISS AIR FORCE BASE, NEW YORK 13441

This report has been reviewed by the RADC Information Office (OI) and is releasable to the National Technical Information Service (NTIS). At NTIS it will be releasable to the general public, including foreign nations.

This report has been reviewed and approved for publication.

APPROVED: *Jacob Scherer*

JACOB SCHERER
Project Engineer

APPROVED: *Joseph J. Naresky*

JOSEPH J. NARESKY
Chief, Reliability & Compatibility Division

FOR THE COMMANDER: *John P. Huss*

JOHN P. HUSS
Acting Chief, Plans Office

Do not return this copy. Retain or destroy.

9 Technical rept.,

UNCLASSIFIED

SECURITY CLASSIFICATION OF THIS PAGE (When Data Entered)

REPORT DOCUMENTATION PAGE

READ INSTRUCTIONS BEFORE COMPLETING FORM

1. REPORT NUMBER: 18 RADC 19 TR-77-43

2. GOVT ACCESSION NO:

3. RECIPIENT'S CATALOG NUMBER:

4. TITLE (and Subtitle): 6 APPLICATION OF MOM/GTD TECHNIQUES TO SHIPBOARD ANTENNAS.

5. TYPE OF REPORT & PERIOD COVERED: Phase Report

6. PERFORMING ORG. REPORT NUMBER: N/A

7. AUTHOR(s): 10 Dr. Jose Perini, Chien-an Chen

8. CONTRACT OR GRANT NUMBER(s): 15 F30602-75-C-0121

9. PERFORMING ORGANIZATION NAME AND ADDRESS: Syracuse University, Syracuse NY 13210

10. PROGRAM ELEMENT, PROJECT, TASK AREA & WORK UNIT NUMBERS: 95670016

11. CONTROLLING OFFICE NAME AND ADDRESS: Rome Air Development Center (RBC), Griffiss AFB NY 13441

12. REPORT DATE: 11 January 1977

13. NUMBER OF PAGES: 41 12 54p.

14. MONITORING AGENCY NAME & ADDRESS (if different from Controlling Office): Same 16 9567 17 00

15. SECURITY CLASS. (of this report): UNCLASSIFIED

15a. DECLASSIFICATION/DOWNGRADING SCHEDULE: N/A

16. DISTRIBUTION STATEMENT (of this Report)

Approved for public release; distribution unlimited.

17. DISTRIBUTION STATEMENT (of the abstract entered in Block 20, if different from Report)

Same

18. SUPPLEMENTARY NOTES

RADC Project Engineer:
Jacob Scherer (RBC)

19. KEY WORDS (Continue on reverse side if necessary and identify by block number)

Electromagnetic Compatibility
Electromagnetic Fields
Method of Moments
Geometrical Diffraction Techniques

20. ABSTRACT (Continue on reverse side if necessary and identify by block number)

The MOM/GTD technique has been used in this report to calculate the radiation patterns of HF shipboard antennas. The ship model was made progressively more complex so that the effects of different parts of the ship could be assessed.

The results compare very well with measured data for the cases studied.

DD FORM 1 JAN 73 1473 EDITION OF 1 NOV 65 IS OBSOLETE

UNCLASSIFIED

SECURITY CLASSIFICATION OF THIS PAGE (When Data Entered)

406737

UNCLASSIFIED

SECURITY CLASSIFICATION OF THIS PAGE(When Data Entered)

UNCLASSIFIED

SECURITY CLASSIFICATION OF THIS PAGE(When Data Entered)

PREFACE

This effort was conducted by Syracuse University under the sponsorship of the Rome Air Development Center Post-Doctoral Program for the Navy. Mr. Tony Testa of NAVSEC was the task project engineer and provided overall technical direction and guidance. The authors of this report are Dr. Jose Perini and Chien-an Chen.

The RADC Post-Doctoral Program is a cooperative venture between RADC and some sixty-five universities eligible to participate in the program. Syracuse University (Department of Electrical and Computer Engineering), Purdue University (School of Electrical Engineering), Georgia Institute of Technology (School of Electrical Engineering), and State University of New York at Buffalo (Department of Electrical Engineering) act as prime contractor schools with other schools participating via sub-contracts with the prime schools. The U.S. Air Force Academy (Department of Electrical Engineering), Air Force Institute of Technology (Department of Electrical Engineering), and the Naval Post Graduate School (Department of Electrical Engineering) also participate in the program.

The Post-Doctoral Program provides an opportunity for faculty at participating universities to spend up to one year full time on exploratory development and problem-solving efforts with the post-doctorals splitting their time between the customer location and their educational institutions. The program is totally customer-funded with current projects being undertaken for Rome Air Development Center (RADC), Space and Missile Systems Organization (SAMSO), Aeronautical Systems Division (ASD), Electronic Systems Division (ESD), Air Force Avionics Laboratory (AFAL), Foreign Technology Division (FTD), Air Force Weapons Laboratory (AFWL), Armament Development and Test Center (ADTC), Air Force Communications Service (AFCS), Aerospace Defense Command (ADC), Hq USAF, Defense Communications Agency (DCA), Navy, Army, Aerospace Medical Medical Division (AMD), and Federal Aviation Administration (FAA).

Further information about the RADC Post-Doctoral Program can be obtained from Jacob Scherer, RADC/RBC, Griffiss AFB, NY, 13441, telephone AV 587-2543, COMM (315) 330-2543.

TABLE OF CONTENTS

LIST OF FIGURES

LIST OF FIGURES cont.

APPLICATION OF MOM/GTD TECHNIQUES TO SHIPBOARD ANTENNAS

1. INTRODUCTION

In the initial phases of ship design it is important to have a tool to assess the effect of the ship superstructure on the radiation pattern of communication antennas. The accuracies required are of the order of 3 to 6 dB. The purpose of this effort is to study the feasibility of a combination of MOM and GTD to provide this tool.

Moment Methods and GTD

The method of moments (MOM) has proven to be a powerful tool for solving problems of EM radiation, scattering and coupling [1-2] for bodies a few wavelengths in size. Numerous EM problems have been solved by MOM in spite of the complexity of the scattering structures. The development of body of revolution algorithms has extended the applicability of the method into some problems involving somewhat larger structures. However, for most large problems, MOM requires excessive amounts of computer storage and running time severely restricting its use. The Geometrical Theory of Diffraction (GTD) [3-17] can be effectively applied to large EM problems but it requires prior knowledge of the current distribution on the exciting structures. By properly combining MOM and GTD, especially in the case of wire antennas, the current distribution can be computed by MOM and then GTD used to take into consideration the reflection and diffraction effects.

In this report, the technique of combining MOM and GTD to solve the problems of antennas mounted on ships is developed based on the ideas of Thiele [3]. A brief description of the formulation is presented in section 2, while the chronological progress made on its use for shipboard antennas is described in section 3. Initially, the simple problems of antennas mounted on finite size conducting ground planes and boxes are analyzed to test and gain confidence in this technique. It is found that the effect of edges on the antenna current distribution is usually of secondary importance compared to that of the antenna self and mutual coupling. But the effect of edges is very important to the radiation pattern, especially in shadow regions.

Next MOM/GTD is applied to the calculation of the radiation pattern of the PF shipboard Twin-Fan Antenna. Based on the experience gained in the work with finite size ground planes and boxes, the effects of edges on the current distribution are neglected resulting in considerable savings in computer running time. The current distribution on the antennas is obtained by MOM alone, considering the antennas and parasite structures mounted on an infinite ground plane. The radiation pattern then includes the direct field from the antennas and parasite structures, the diffraction fields from edges, the multi-diffraction fields between edges, and the reflected field from the conducting surface. The computations in this section are quite involved because of the complexity of the ship structure.

Models for the ship's superstructure are then developed and reasonably good results are obtained even with the simplest ones. The Twin-Fan Antenna is also replaced by a simplified structure. It is found that the effects of the side edges of the ship and bridge are most important in the azimuthal range from 50° to 110° from the bow because of their close proximity to the antenna. More detailed models in these areas are then developed to improve the simulation results. Finally, it is found that the radiation pattern has a sharp change in both the forward and backward directions when the frequency changes. This required a further refined model which includes all other antennas on the ship. Presently, an open circuit at the feed point for these antennas has been assumed since a high mismatch is expected for the frequencies used in the calculation. Radiation patterns for this model have been calculated at frequencies of 5 MHz and 6 MHz for small elevation angles. The results are quite good.

This report is a chronological summary of the progress of this research effort during the past year. The model which has been developed is fairly good and has produced very encouraging results. However, the model still does not include the effects of the finite conductivity sea, the presence of structural details such as rails, safety boats, etc. These will be our main goals in next year's effort while exercising the present models in a larger number of problems to gain confidence and familiarity with it.

2. FORMULATION

Method of Moments

For the case of wire antennas or wire grids, the integral equation for the current in the wires is reduced to a system of linear equations. This is done by dividing the antenna into sections and representing the current by local orthogonal functions such as pulses, triangles, etc. with unknown amplitudes and phases. By imposing the appropriate boundary conditions in as many points along the wires as there are expansion functions, the following system of linear equations results: [1]

$$\sum_{n=1}^{N} Z_{mn} I_n = E_m$$

where $m = 1, 2, \ldots, N$

N = the number of subsections on the wires

I_n = coefficient of the expansion function on the nth subsection

Z_{mn} = mutual impedance between the mth and nth subsections. This is the voltage produced at subsection m when one ampere of current is applied at subsection n.

E_m = the excitation at the mth subsection.

Note that all the above variables are complex numbers. Several techniques can be applied to solve this system of equations and find the current distribution.

GTD

Assume that $\vec{E}^{in}$ is the incident E-field from the source and $\vec{E}^{d}$ is the diffracted field from the edge (Fig. 1). Then $\vec{E}^{in}$ and $\vec{E}^{d}$ are related by [4]

$$\vec{E}^{d}(S) = \vec{E}^{in}(Q_E) \cdot \vec{D}_E(\hat{S},\hat{I}) \cdot A(s) e^{-jks}$$

where Q_E is the diffraction point on the edge which is determined by Fermat's principle, and $\vec{D}_E(\hat{S},\hat{I})$ is the Dyadic diffraction coefficient defined as

$$\vec{D}_E(\hat{S},\hat{I}) = \begin{pmatrix} -V_B^- & 0 \\ 0 & -V_B^+ \end{pmatrix} \frac{\sqrt{L}\, e^{jkL}}{\sin \beta_o}$$

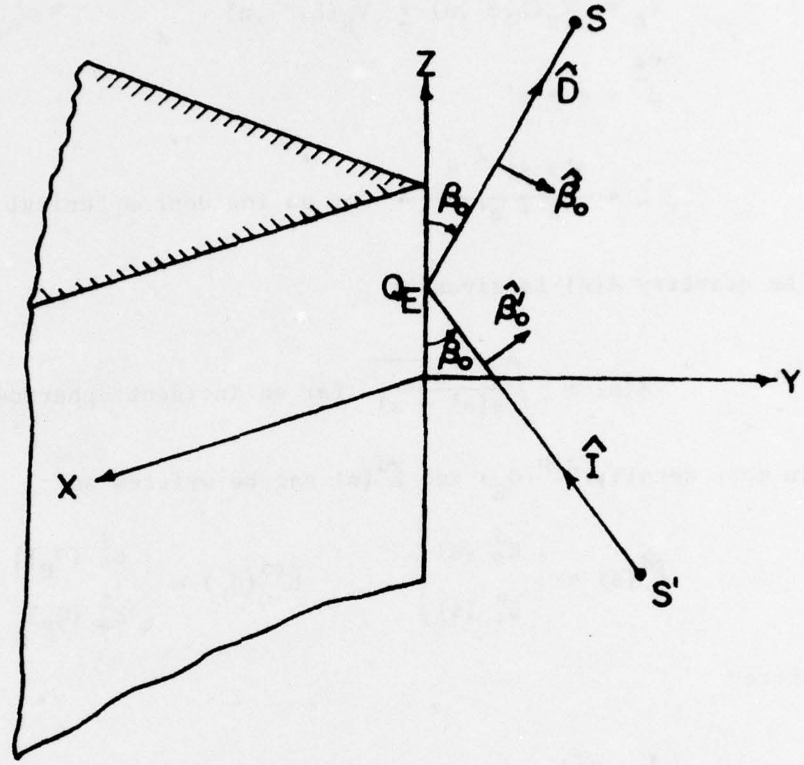
S
$\hat{D}$
Z
$\hat{\beta}_o$
β_o
Q_E
$\hat{\beta}'_o$
β_o
Y
$\hat{I}$
X
S'

FIG. 1

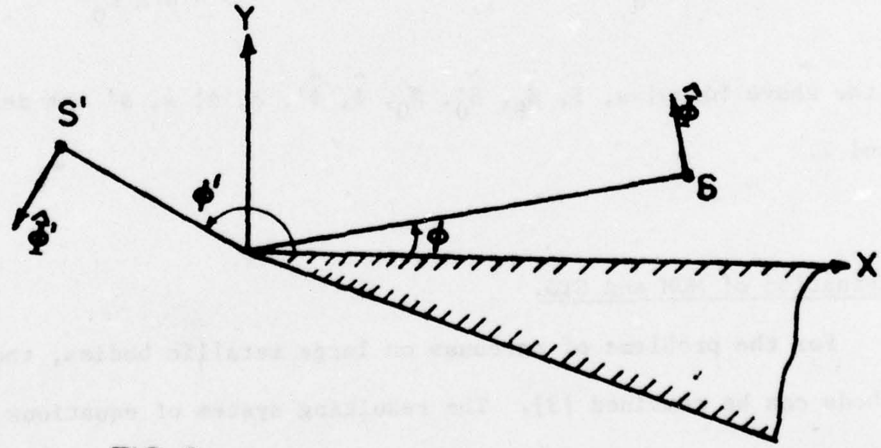
Y
S'
$\hat{\phi}$
S
ϕ'
ϕ
X
$\hat{\phi}'$

FIG. 2

where

$$V_B^{\pm} = V_B(L,\beta^-,n) \pm V_B(L,\beta^+,n)$$

$$\beta^{\pm} = \phi \pm \phi'$$

$$L = \frac{s's \sin^2 \beta_o}{s + s'} \quad \text{for an incident spherical wave}$$

The quantity A(s) is given by

$$A(s) = \sqrt{\frac{s'}{s(s' + s)}} \quad \text{for an incident spherical wave.}$$

In more detail, $\vec{E}^{in}(Q_E)$ and $\vec{E}^d(s)$ can be written as

$$\vec{E}^d(s) = \begin{bmatrix} E^d_{\parallel}(s) \\ E^d_{\perp}(s) \end{bmatrix} \qquad \vec{E}^{in}(Q_E) = \begin{bmatrix} E^i_{\parallel}(Q_E) \\ E^i_{\perp}(Q_E) \end{bmatrix}$$

where

$$E_{\parallel}^i = \vec{E}^{in} \cdot \hat{\beta}_0' \qquad\qquad E_{\parallel}^d(s) = \vec{E}^d \cdot \hat{\beta}_0$$

$$E_{\perp}^i = \vec{E}^{in} \cdot \hat{\phi}' \qquad \text{and} \qquad E_{\perp}^d(s) = \vec{E}^d \cdot \hat{\Phi}$$

$$\hat{\Phi}' = \hat{I} \times \hat{\beta}_0' \qquad\qquad \hat{\Phi} = \hat{D} \times \hat{\beta}_0$$

In the above formulas, $\hat{I}$, $\hat{\beta}_0$, $\hat{\beta}_0'$, β_0, $\hat{\Phi}$, $\hat{\Phi}'$, ϕ, ϕ', s, s' are defined in Figs. 1 and 2.

<u>Combination of MOM and GTD</u>.

For the problems of antennas on large metallic bodies, the above two methods can be combined [3]. The resulting system of equations is

$$\sum_{n=1}^{N} Z'_{mn} I'_n = E_m$$

where m = 1, 2, ..., N.

The new impedance elements Z'_{mn} are

$$Z'_{mn} = Z_{mn} + (Z_{mn})^{GTD} + (Z_{mn})^{image}$$

where Z_{mn} is the conventional MOM mutual impedance, $(Z_{mn})^{GTD}$ is the contribution to the mutual impedance due to the diffraction fields and $(Z_{mn})^{image}$ is the contribution to the mutual impedance due to the reflections from the metallic surfaces.

The Radiation Field

After solving the system of linear equations for the current distribution on the antenna, the radiation field of the antenna in the presence of the metallic body is then computed as

$$E_{rad} = E_{antenna} + E_{image} + E_{GTD}$$

where

$E_{antenna}$ is the field due to the current on the antenna only.

E_{image} is the field reflected from the metallic body.

E_{GTD} is the field diffracted from the edges of the metallic body.

3. APPLICATION OF GTD AND MOM TO SOME PROBLEMS

The formulation of Section 2 has been verified by comparing it with some of Burnside's and Thiele's results [3],[4]. In the next sections we will discuss the numerical results obtained by applying this technique to the following problems:

(a) Antennas (one or more) on a finite ground plane.

(b) Antennas (one or more) on a conducting box.

(c) The Shipboard Twin-Fan Antenna.

Antennas on Finite Ground Plane

In Fig. 3a, a $\lambda/4$ monopole is located on a finite size conducting plane[†] with Lx and Ly as variables. The antenna itself is treated by MOM. Five subsections with piecewise sinusoidal expansion functions and pulse testing functions are used [1].[*] The mutual coupling between the antenna and edges is treated by GTD [4]. For comparison, the monopole located on an infinite conducting plane is shown in Fig. 3b. The input impedance and the current magnitude of each subsection of Figs. 3a and b for different size conducting planes are shown in Table 1. It is noted that the antenna input resistance increases and the current amplitude decreases as the conducting plane gets smaller. Note also, by comparing the first column with the others that the effect of the edges on the current distribution of a simple monopole is small indeed.

The radiation patterns $|E(\theta)|$ corresponding to the cases in Table 1 are shown in Figs. 4 and 5. In both figures, there is a dotted-line plot which is the radiation pattern of a monopole on a finite size ground plane without considering the diffraction from edges. From the comparison of these two curves it can be seen that the effect of the edges is very important

---

*Testing functions are the same type of local orthogonal functions used to expand the current distributions. They are used to expand the excitation and this process is tantamount to imposing the appropriate boundary condition at each antenna subsection.

†Conducting plane throughout this report means perfectly conducting plane.

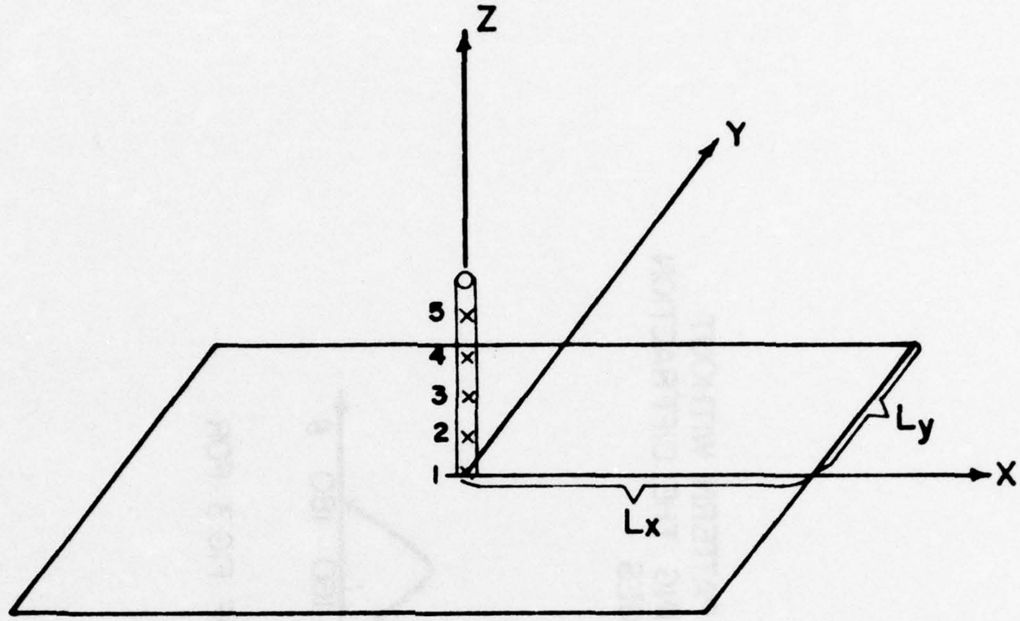

FIG. 3-(a) λ/4 MONOPOLE OVER FINITE CONDUCTING PLANE

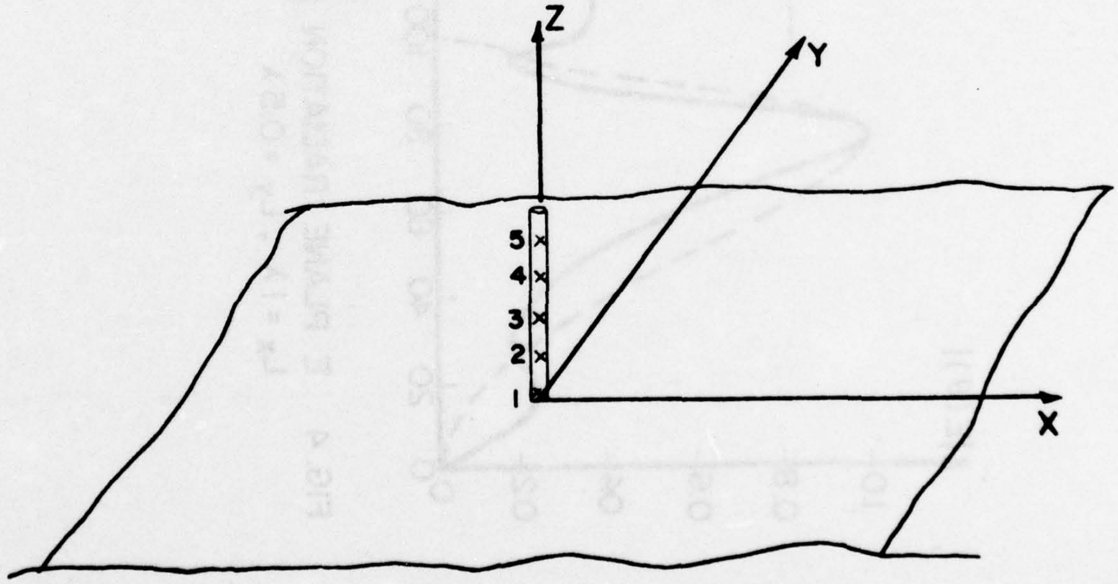

FIG. 3-(b) λ/4 MONOPOLE OVER INFINITE CONDUCTING PLANE

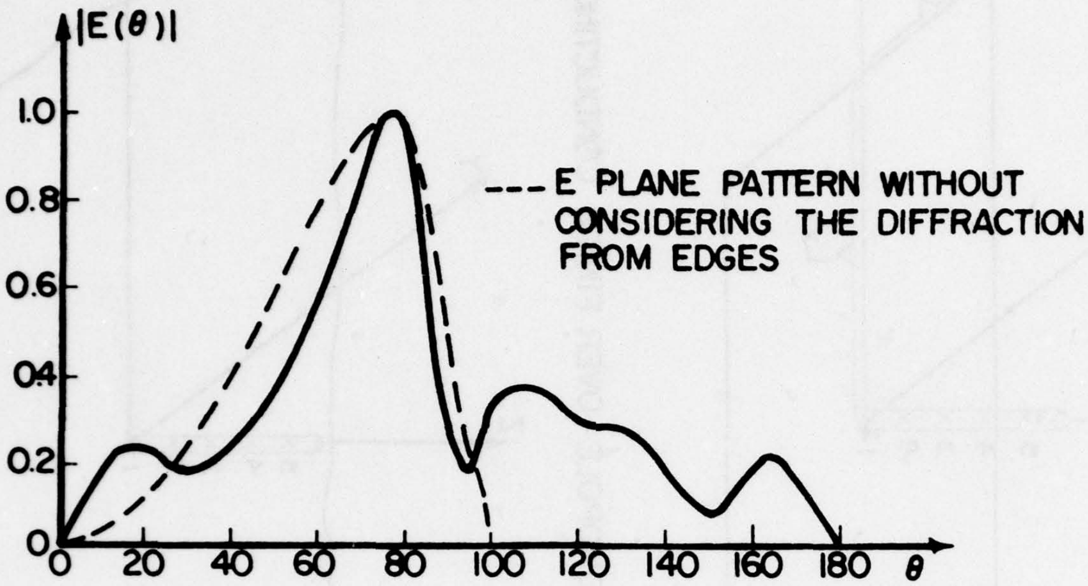

FIG. 4 E PLANE RADIATION PATTERN OF FIG.3 FOR $L_x = 1\lambda$, $L_y = 0.5\lambda$

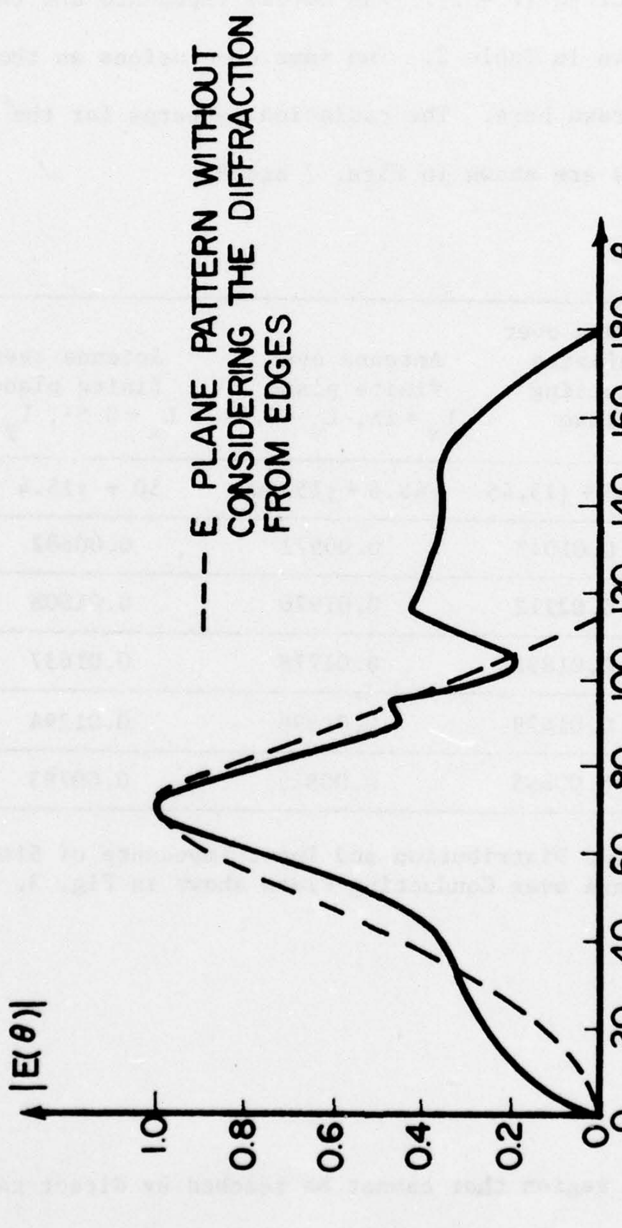

FIG. 5 E PLANE RADIATION PATTERN OF FIG. 3 FOR $L_x = 0.5\lambda$, $L_y = 0.5\lambda$

especially in the shadow region.*

In Fig. 6, two monopoles are located on a finite size conducting plane. The distance between the two antennas is one wavelength. The antennas are equally excited (v = 1). The mutual impedance and the current distributions are shown in Table 2. The same conclusions as those drawn from Table 1 can be drawn here. The radiation patterns for the different size conducting planes are shown in Figs. 7 and 8.

		Antenna over infinite conducting plane	Antenna over finite plane $L_x = 1\lambda$, $L_y = 0.5\lambda$	Antenna over finite plane $L_x = 0.5\lambda$, $L_y = 0.5\lambda$
Input Impedance		45.35 + j15.45	48.6 + j15.66	50 + j15.4
Current (mag) Distribution (correspon-ding to the same location in Fig. 3.)	1	0.01043	0.00971	0.00882
	2	0.02112	0.01976	0.01808
	3	0.01892	0.01778	0.01637
	4	0.01479	0.01396	0.01294
	5	0.00895	0.00849	0.00793

Table 1. Current Distribution and Input Impedance of Single Antenna over Conducting Plane shown in Fig. 3.

---
*Shadow region is the region that cannot be reached by direct rays from the source.

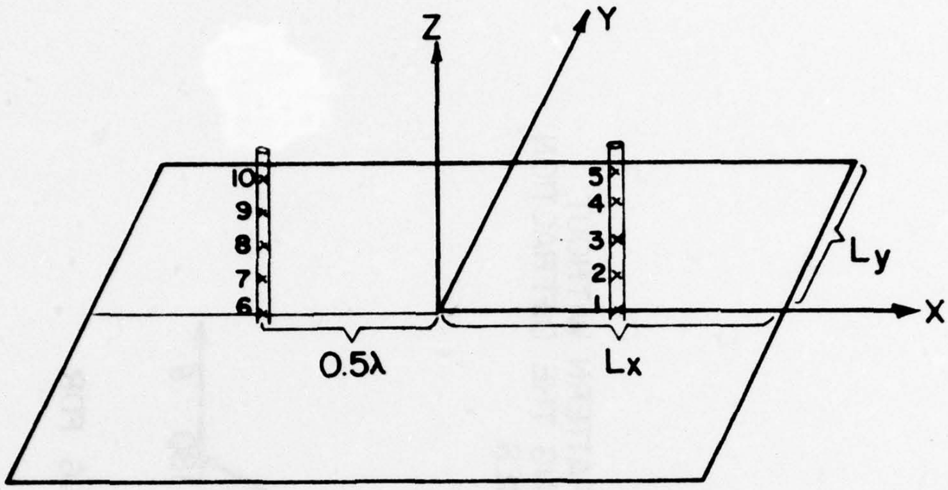

FIG.6-(a) TWO λ/4 MONOPOLES LOCATED OVER FINITE CONDUCTING PLANE

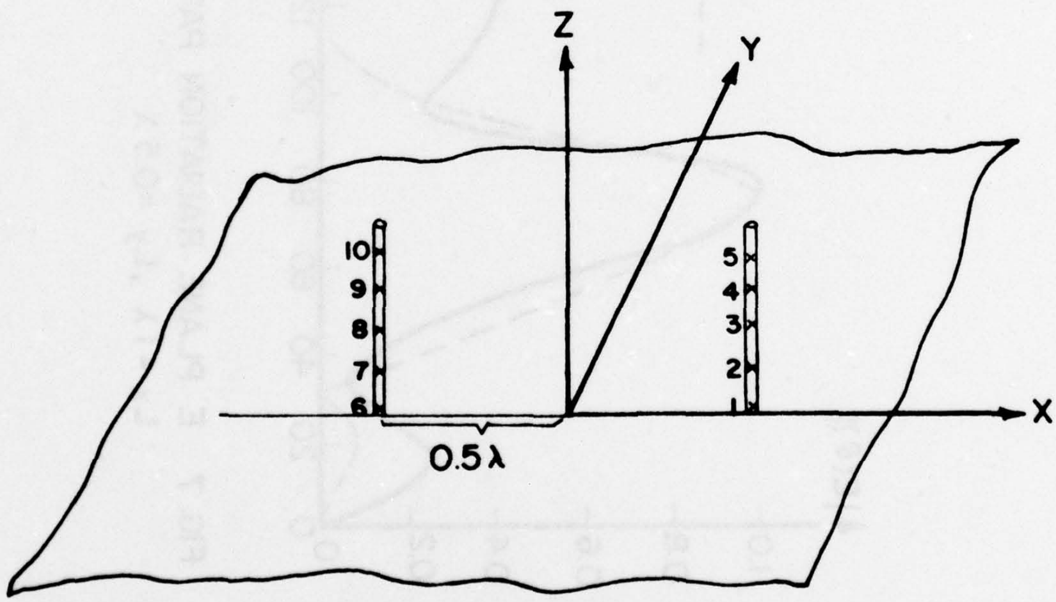

FIG.6-(b) TWO λ/4 MONOPOLES LOCATED OVER INFINITE CONDUCTING PLANE

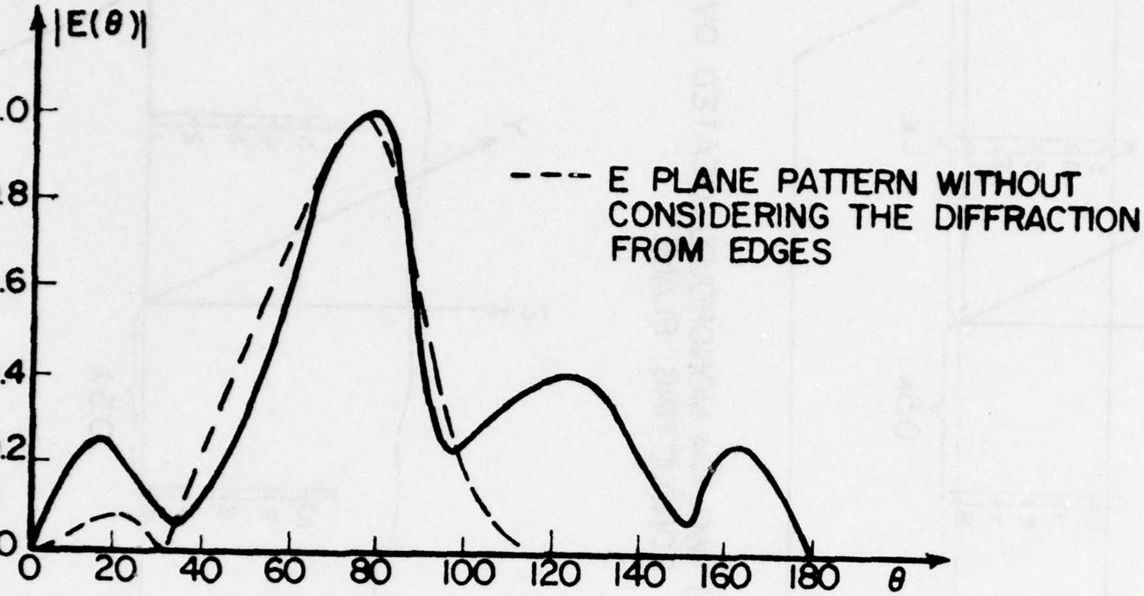

FIG. 7 E PLANE RADIATION PATTERN OF FIG.6 FOR $L_x = 1\lambda$, $L_y = 0.5\lambda$

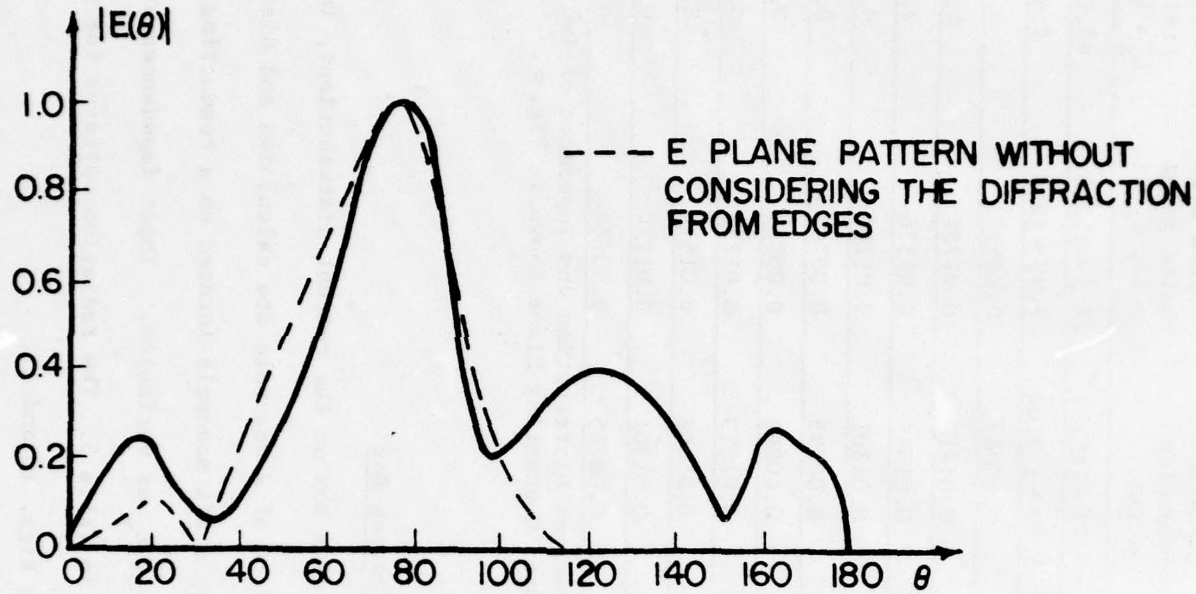

FIG.8 E PLANE RADIATION PATTERN OF FIG.6 FOR $L_x = 1.\lambda$, $L_y = 1.\lambda$

		Antenna over infinite conducting plane	Antenna over finite plane $L_x = 1\lambda$, $L_y = 1\lambda$	Antenna over finite Plane $L_x = 1\lambda$, $L_y = 0.5\lambda$
Input impedance		45.73 + j15.71	47.5 + j15.8	48.17 + j15.9
Mutual impedance		5.93 + j 9.62	7.35 + j8.9	5.49 + j8.429
Current (mag) distribution (correspon-ding to the same location in Fig. 6.)	1	0.00869	0.00823	0.00777
	2	0.01813	0.01728	0.01628
	3	0.01647	0.01576	0.01486
	4	0.01301	0.01250	0.01182
	5	0.00795	0.00767	0.00728
	6	0.00869	0.00823	0.00777
	7	0.01813	0.01728	0.01628
	8	0.01647	0.01576	0.01486
	9	0.01301	0.01250	0.01182
	10	0.00795	0.00767	0.00728

Table 2. Current Distribution and Impedance of Two Antennas Over Conducting Plane Shown in Fig. 6 .

Antennas on a Conducting Box

The effects of a box on the current distributions, input impedances, and radiation pattern of a monopole are calculated and discussed in this section. Fig. 9 *shows a* $\lambda/4$ *monopole located on a* conducting box of infinite height and with L_x, L_y as variables. Input impedances and current distributions are shown in Table 3. The radiation patterns for boxes of different sizes are shown in Figs. 10 and 11.

The same conclusions drawn in the previous section can be drawn here. That is, the effect of the edges on the current distribution is very small

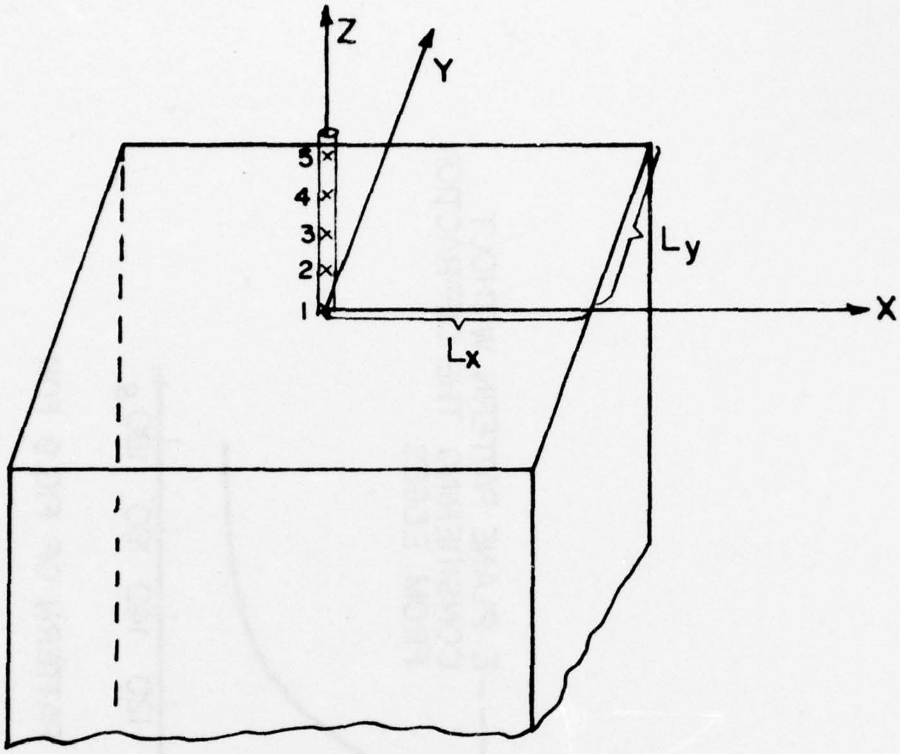

FIG. 9-(a) λ/4 MONOPOLE LOCATED OVER A CONDUCTING BOX

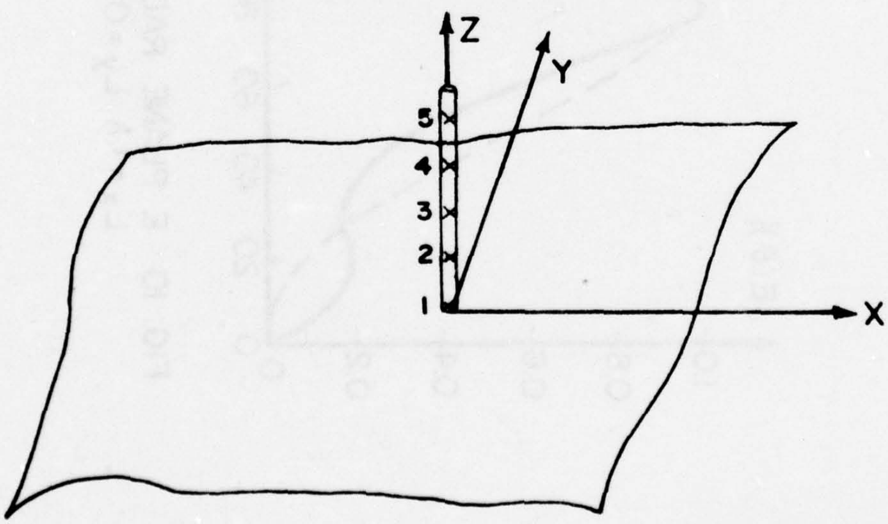

FIG. 9-(b) λ/4 MONOPOLE LOCATED OVER A CONDUCTING PLANE

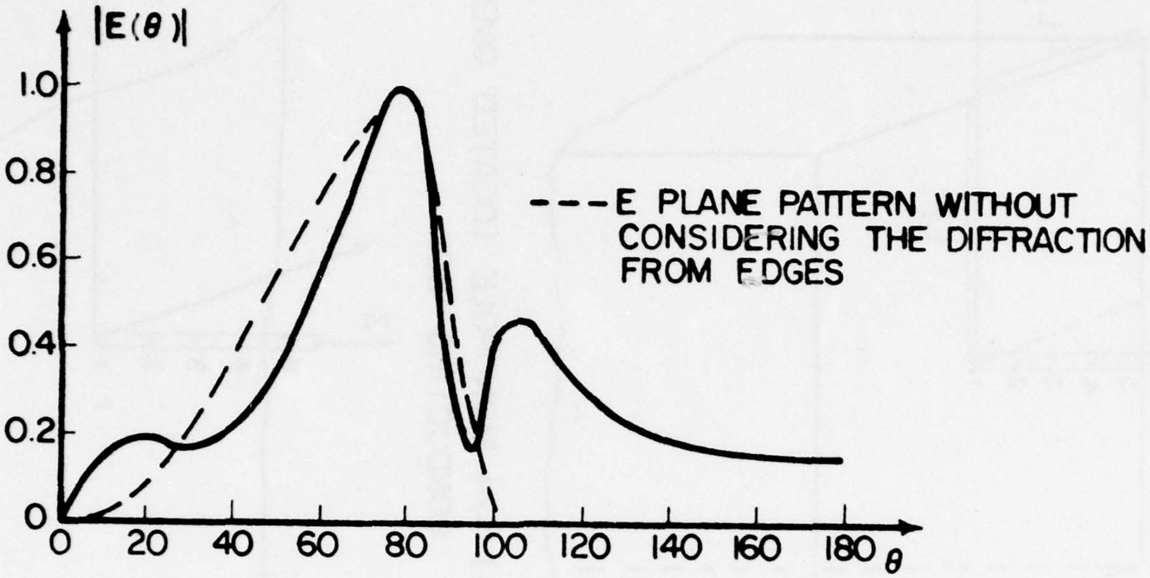

FIG. 10 E PLANE RADIATION PATTERN OF FIG. 9 FOR $L_x = 1.\lambda$, $L_y = 0.5\lambda$

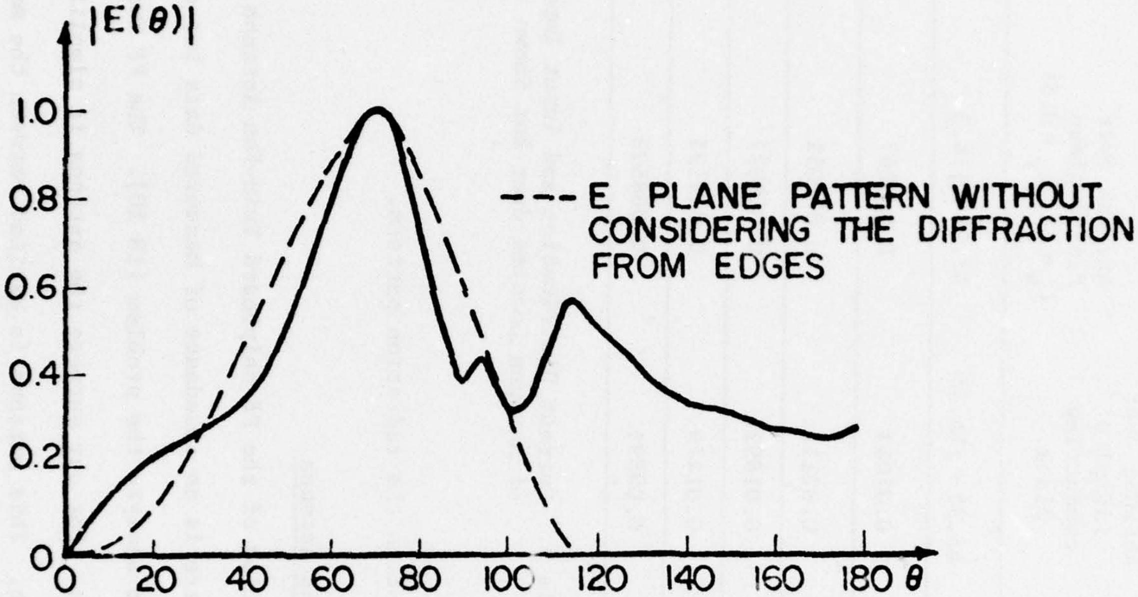

FIG. 11 E PLANE RADIATION PATTERN OF FIG. 9 FOR $L_x = 0.5\lambda$, $L_y = 0.5\lambda$

		Antenna over infinite conducting plane	Antenna over finite plane $L_x = 1\lambda$, $L_y = 0.5\lambda$	Antenna over finite plane $L_x = 0.5\lambda$, $L_y = 0.5\lambda$
Input impedance		45.35 + j15.45	47.98 + j16.3	50.16 + j17.48
Current (mag) distribution (correspon-ding to the same location in Fig. 9)	1	0.01043	0.009867	0.009147
	2	0.02112	0.020051	0.018698
	3	0.01892	0.018027	0.016892
	4	0.01479	0.014135	0.013314
	5	0.00895	0.008593	0.008141

Table 3. Current Distribution and Input Impedance of Antenna Located over Box Shown in Fig. 9.

but very important in the radiation pattern.

Shipboard Twin-Fan Antenna

The simulation of the PF Shipboard Twin-Fan Antenna is the main goal of this report. There is an abundance of measured data but only a few attempts have been made to analyze the problem [18-20]. The PF Twin-Fan antenna is shown in Fig. 12a. For our purpose the antenna is simplified to the model shown in Fig. 12b. This antenna is excited between the main mast and the horizontal wire as shown in Fig. 12b and its radiation pattern, when on an infinite ground plane, is shown in Fig. 13. For the frequency of 4.6 MHz, the Twin-Fan Antenna is so small in wavelength that it behaves like a small

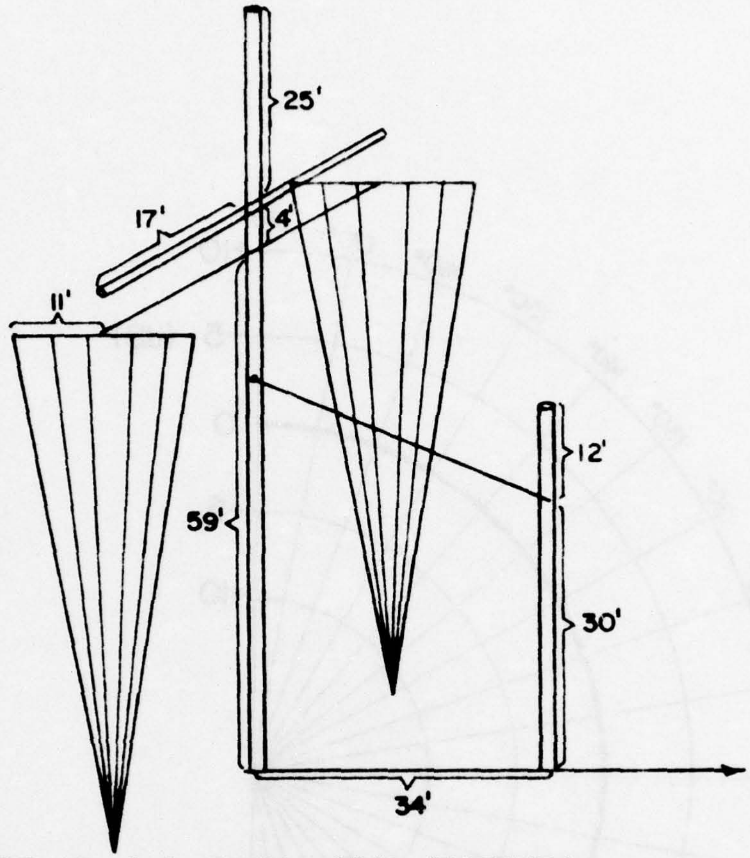

FIG. 12 - (a) TWIN FAN ANTENNA

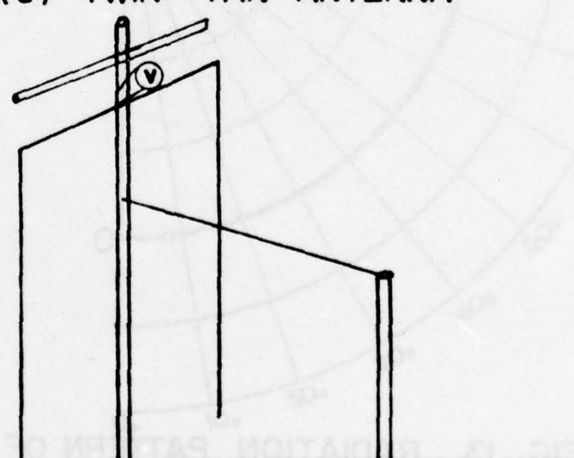

FIG. 12 - (b) THE MODEL FOR TWIN-FAN ANTENNA

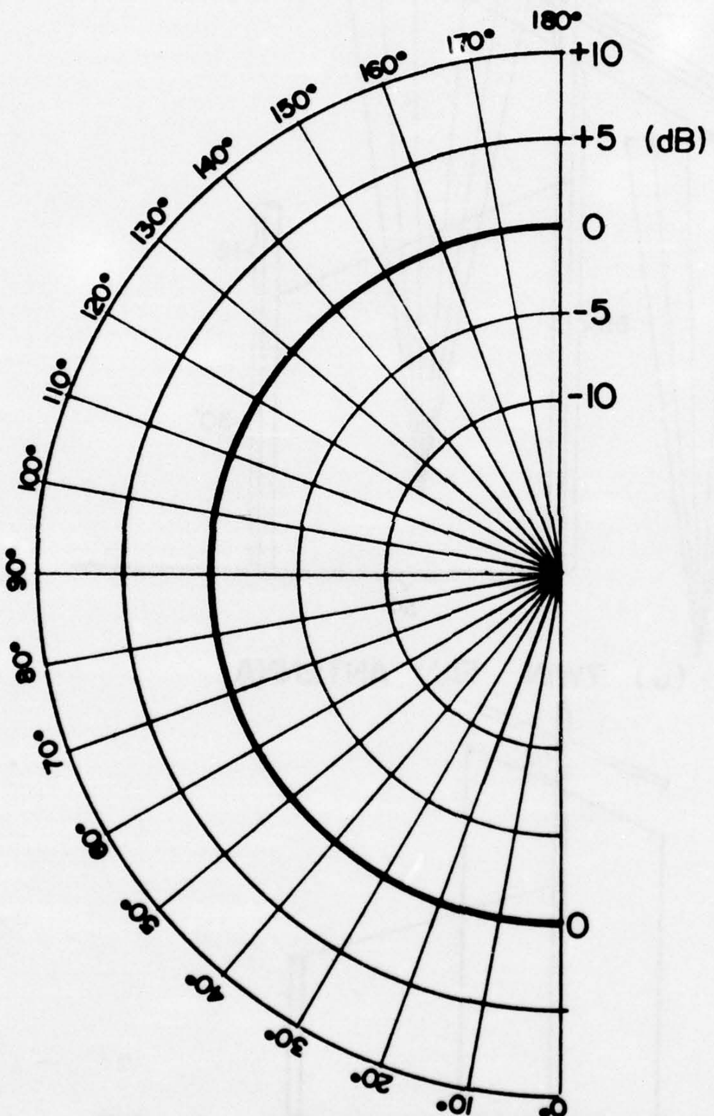

FIG. 13 RADIATION PATTERN OF TWIN FAN ANTENNA OVER INFINITE CONDUCTING PLANE AT 6° ELEVATION AND f = 4.6MHz (VERTICAL POLARIZATION)

monopole, hence the omnidirectional pattern.

When the Twin-Fan Antenna is located on the PF ship, the effects of the complicated neighboring structures make the radiation pattern different from that of a simple monopole. The radiation pattern which will be simulated in this section is pattern #103 (4.6 MHz), Antenna (2-1), Vertical Polarization at 6° elevation angle from:

Preliminary Engineering Report (5 March 1973)

Isolation and Radiation Pattern Data

1:48 Scale PF Ship Model Analysis

Sm. No. 72-DECO-5

This radiation pattern was also used by Raschke in his report [18].

As it can be seen in the development of Section 2 relating to the combination of GTD and MOM, if the terms $(Z_{mn})^{GTD}$ are included (the contribution of diffraction effects in the current distribution) then N^2 extra calculations are required, where N is the number of subsections in the antennas. This will require a great deal of computation time when N is large. However, from the results of Tables 1, 2, and 3 of Section 3, we see that the effect of the diffraction fields from the edges on the current distribution is very small. Therefore, the current distribution on the Twin Fan Antenna will be obtained by MOM considering the antenna over an infinite ground plane. In the radiation pattern the diffracted and reflected fields are all considered.

In order to gain insight in the problem, it was decided to start with very simple models which became progressively more complex as the comparison with experimental results required. Initially, we observe that the side edges of the ship and the bridge are much closer to the antenna than any other structure. The model shown in Fig. 14 was then considered first. The Twin Fan Antenna is located in the center and the edges are extended to infinity in both directions. The current distribution on the Twin Fan Antenna is first calculated by MOM. Many calculations have been made for different parameters of the Twin Fan Antenna and by considering different sets of multiple diffraction from the edges. Some of these radiation patterns are shown in Fig. 17, where the x's represent measured data from the report referred to above. It is interesting to note that the result of this most simple model has the correct general shape except for a large error in the forward direction.

The parameters for the Twin Fan Antenna used for these calculations were in part derived from the report and in part from pictures. They are the following: the distance from the base to the feed point is 59 feet, the distance between the two transmission lines, shown in Fig. 12a is 4 feet, the distance that the main mast extends above the transmission lines is 25 feet, the width of the antenna is 34 feet, the distance between the two masts is 30 feet, the height of the second mast is 42 feet, the radius for the two masts is 0.3 meters, the radius of the wire is 0.01 meter, and the radius of the yard arm is 0.1 meter.

Using the above set of parameters for the Twin Fan Antenna and the model of Fig. 14, the radiation pattern (vertically polarized field) is shown in Fig. 18 for 6° elevation and f = 4.6 MHz. From a comparison of this radiation pattern with measured data (the x's), we note that there is a large error in the forward direction. It is also interesting to note that the edges of the ship and bridge are the main factors in the radiation

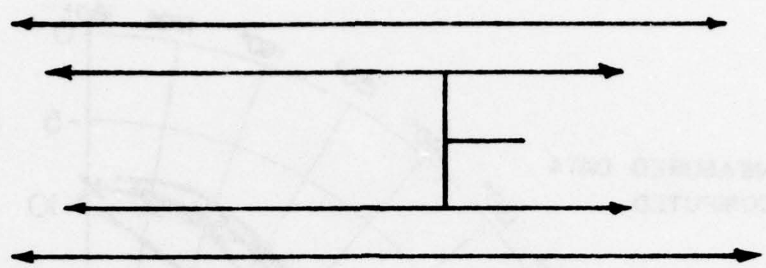

FIG. 14 THE MODEL FOR SHIP AND TWIN FAN ANTENNA

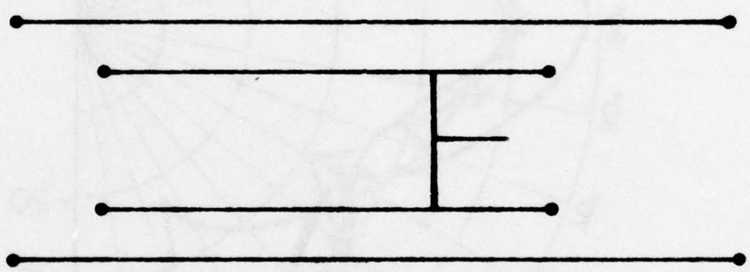

FIG. 15 THE MODEL FOR SHIP AND TWIN FAN ANTENNA

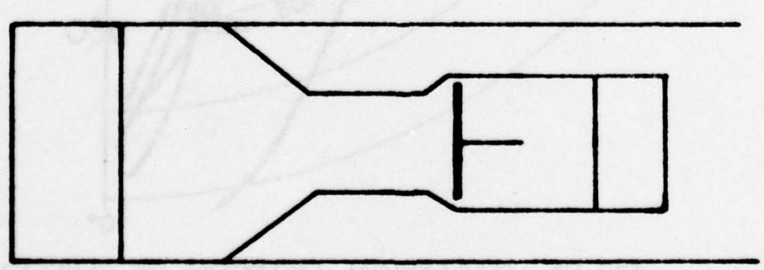

FIG. 16 THE MODEL FOR SHIP AND TWIN FAN ANTENNA

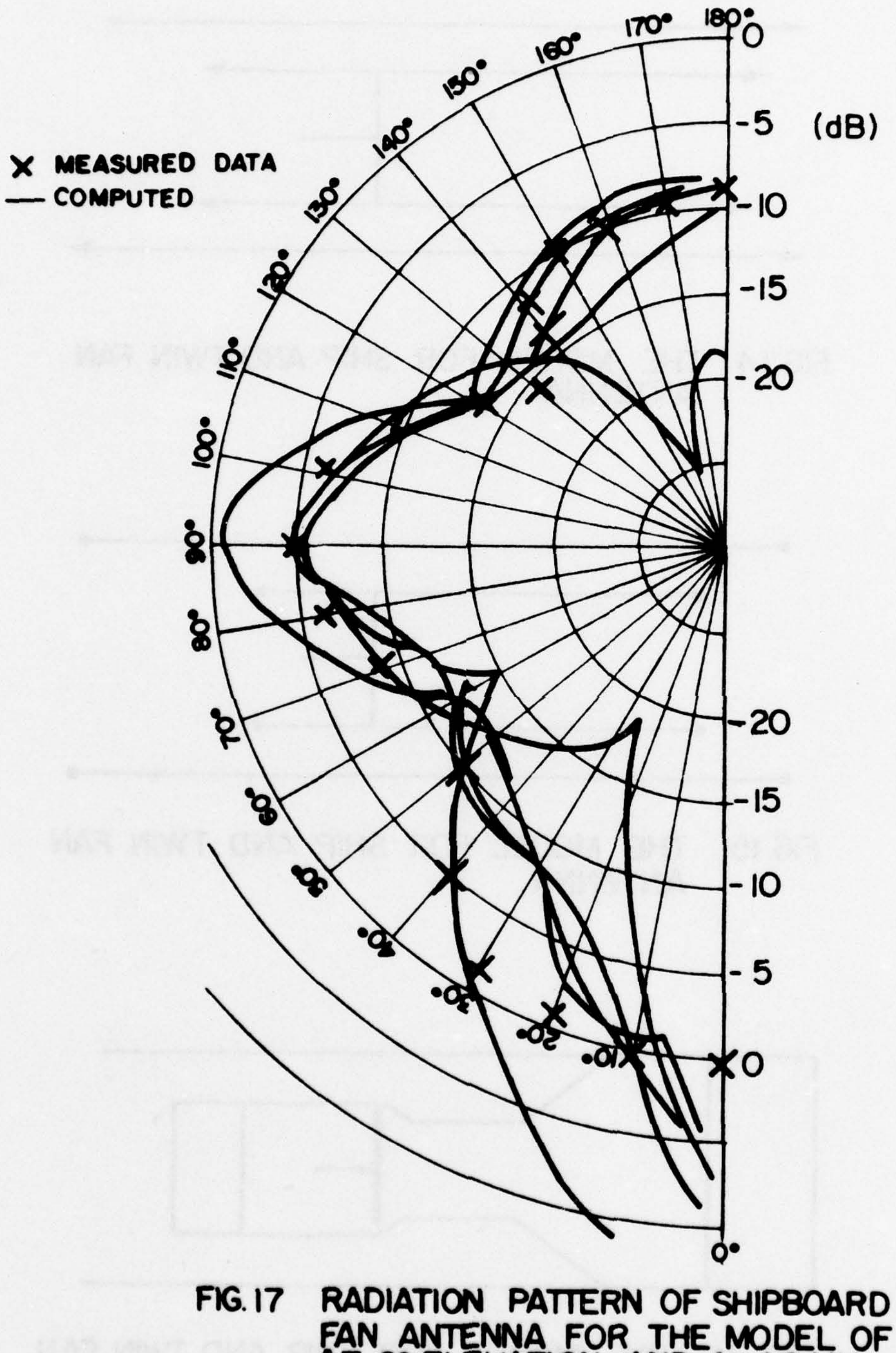

FIG. 17 RADIATION PATTERN OF SHIPBOARD TWIN FAN ANTENNA FOR THE MODEL OF FIG. 14 AT 6° ELEVATION AND f = 4.6 MHz (VERTICAL POLARIZATION)

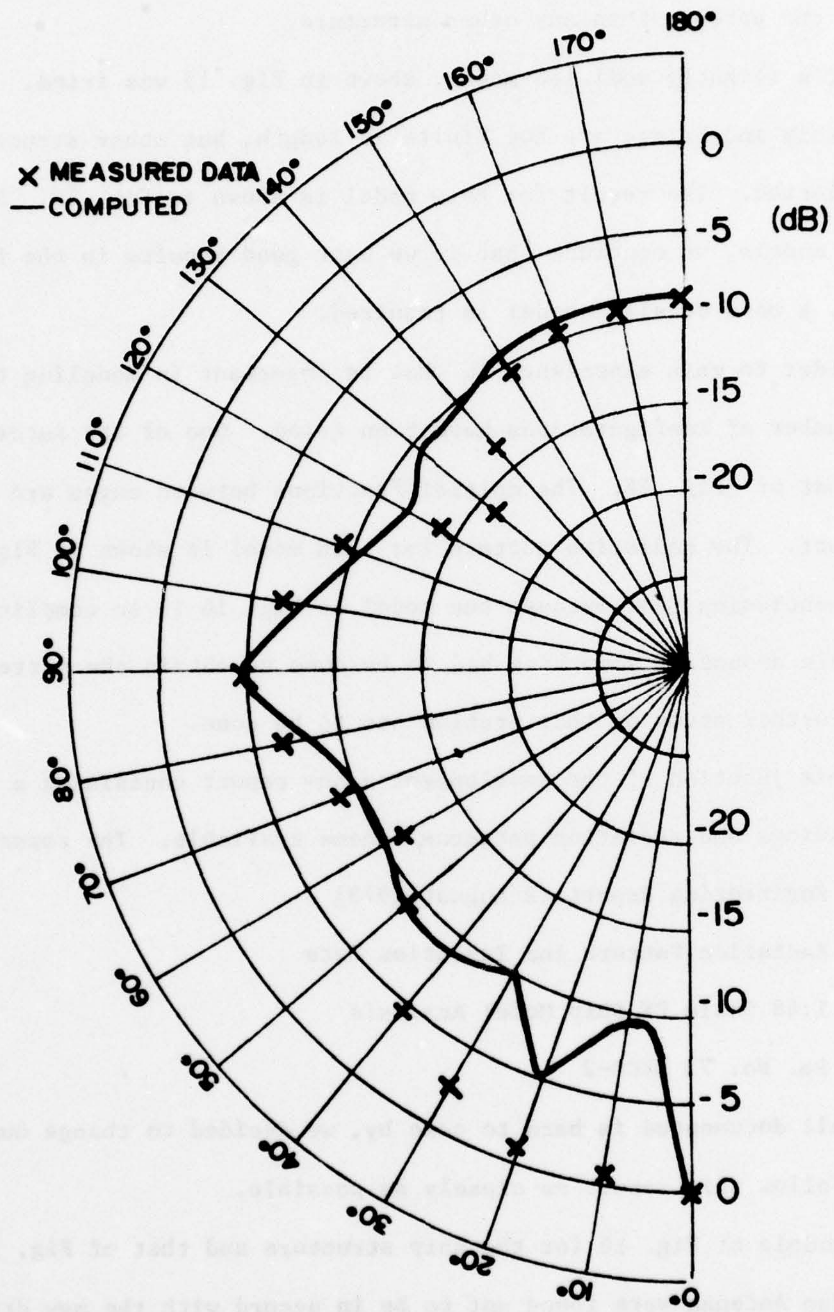

FIG. 18 RADIATION PATTERN OF SHIPBOARD TWIN FAN ANTENNA FOR THE MODEL OF FIG. 14 AT 6° ELEVATION AND f = 4.6 MHz (VERTICAL POLARIZATION)

pattern for ϕ = 50° to 160°. The reason for this is that these edges are closer to the antenna than any other structure.

Next, a slightly modified model, shown in Fig. 15 was tried. The edges of ship and bridge are now finite in length, but other structures are still neglected. The result for this model is shown in Fig. 19. From the above two models, we conclude that if we want good results in the forward direction, a more detailed model is required.

In order to gain experience in what is important in modeling the ship, a large number of configurations have been tried. One of the successful ones is that of Fig. 16. The multidiffractions between edges are taken into account. The radiation pattern for this model is shown in Fig. 20. It is worth mentioning that because the model of Fig. 16 is so complicated, a considerable amount of smoothing had to be done to obtain the pattern presented. Further study on this problem has to be done.

At this junction of the development a new report containing a "complete" set of drawings and radiation patterns became available. The report is:

Engineering Report (2 August 1973)
Radiation Pattern and Isolation Data
1:48 Scale PF Ship Model Analysis
Sm. No. 73 DECO-2

As data well documented is hard to come by, we decided to change our pro grams to follow this report as closely as possible.

The models of Fig. 16 for the ship structure and that of Fig. 12b for the Twin Fan Antenna were found not to be in accord with the new drawings and not very good at higher frequencies and higher elevation angles. A

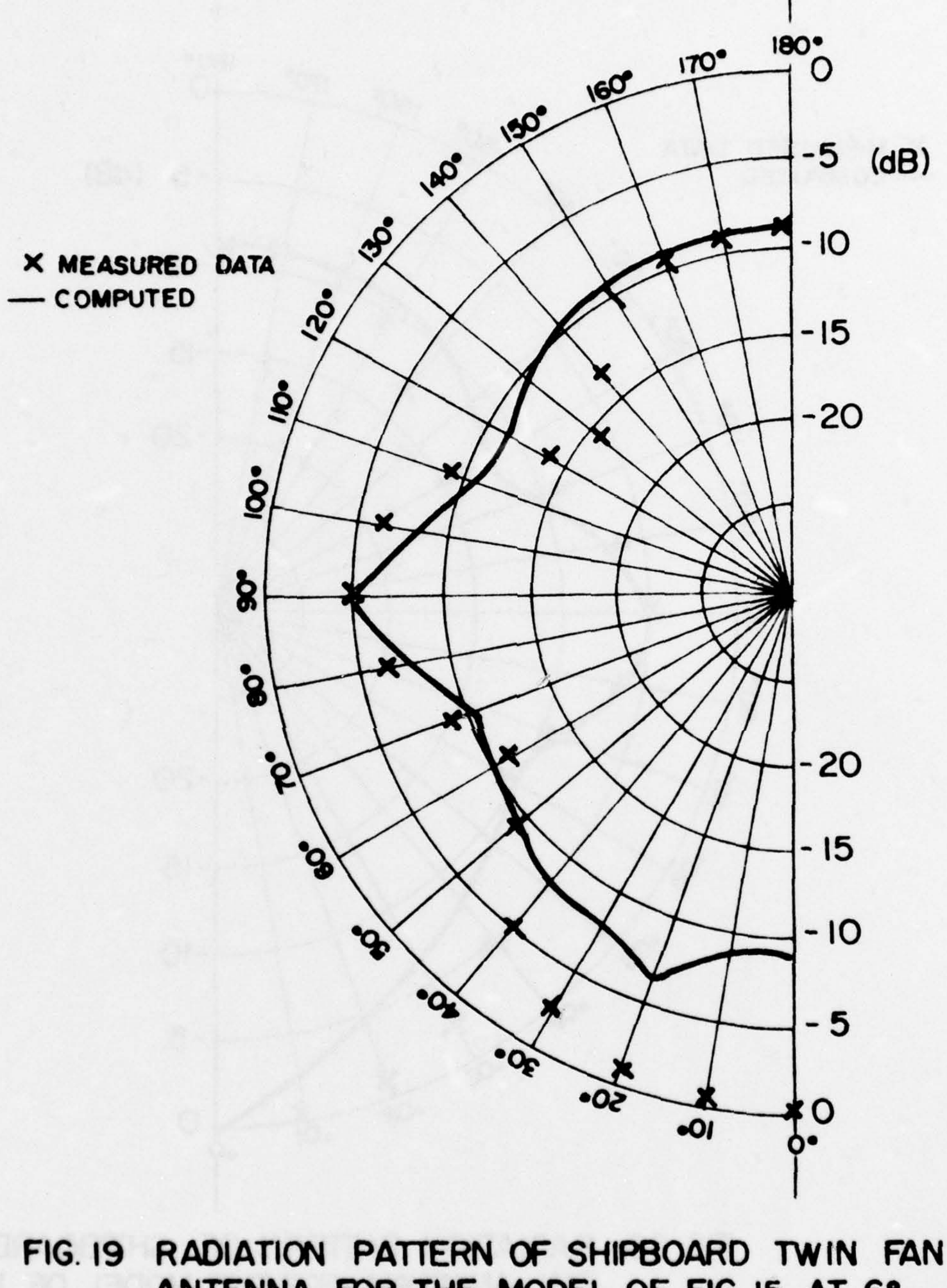

FIG. 19 RADIATION PATTERN OF SHIPBOARD TWIN FAN ANTENNA FOR THE MODEL OF FIG. 15 AT 6° ELEVATION AND f = 4.6 MHz (VERTICAL POLARIZATION)

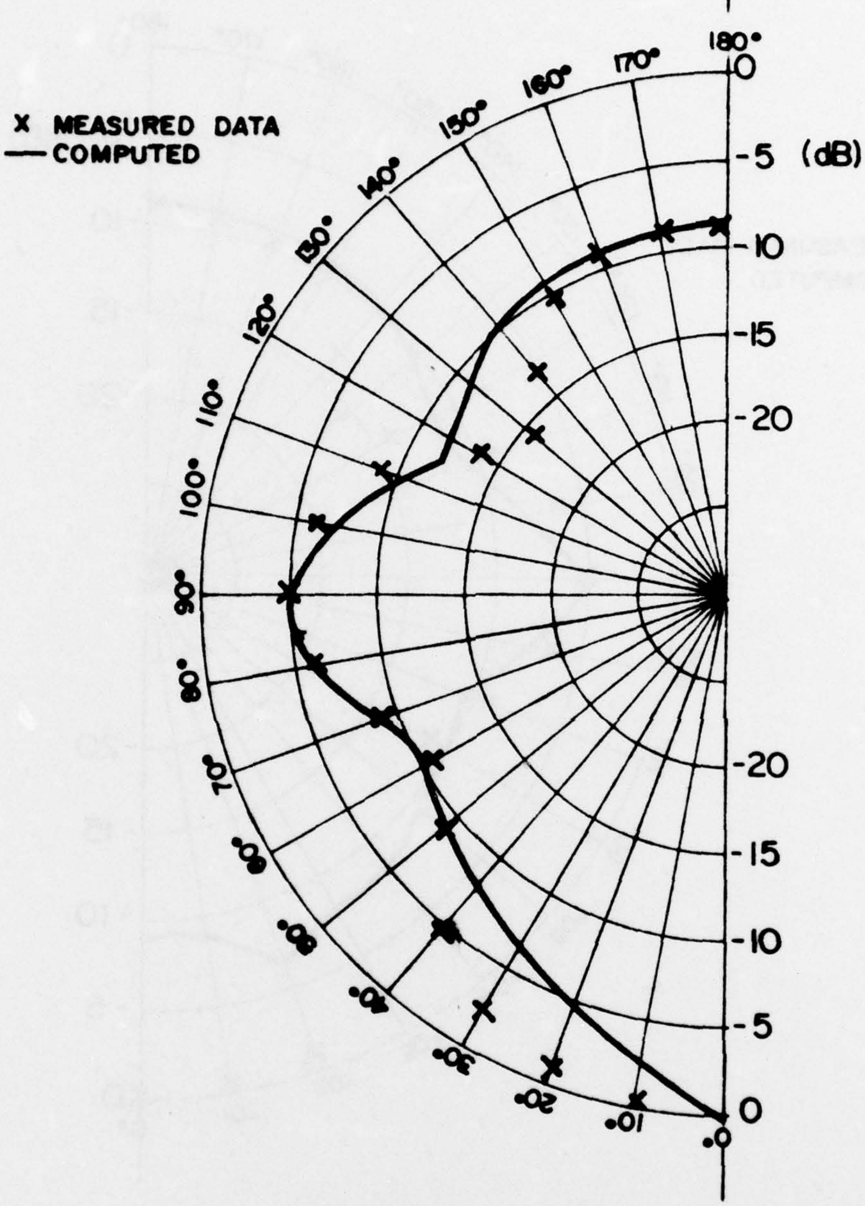

FIG. 20 RADIATION PATTERN OF SHIPBOARD TWIN FAN ANTENNA FOR THE MODEL OF FIG. 16 AT 6° ELEVATION AND f = 4.6 MHz (VERTICAL POLARIZATION)

more complete model, as shown in Fig. 21a, was then developed. In this model, multi-diffractions between edges are considered. The model for the Twin-Fan Antenna is also simplified to that shown in Fig. 21b. The height of the second mast is 42 feet. The distance between the two masts is 34 feet. The radius of the wire between the two masts is 0.02 meters. The radius of the vertical wire is 0.02 meters. After these modifications, radiation patterns for the shipboard Twin-Fan Antenna were computed and are shown in Figs. 22 and 23 at 10° elevation and frequencies of 5 MHz and 6 MHz. It is noted from these two results that there is general agreement in shape, but larger errors in the forward and backward directions.

In the models of ship structure developed above, all other antennas located on the ship were neglected. The existence of those antennas may be important for the radiation pattern even when they are all open-circuited. Fig. 24 shows the actual PF ship model. There are four 35 foot whip antennas and two radar masts with heights of 18 feet and 20 feet. They are shown in Fig. 25. Using this model and assuming that all antennas are open-circuited except the Twin-Fan Antenna, the radiation patterns at 10° elevation and frequencies of 5 MHz and 6 MHz were computed and are shown in Figs. 26 and 27. Agreement with the experimental data is quite good.

CONCLUSION

In this report the feasibility of applying a combination of MOM and GTD to shipboard antennas was studied. The results are surprisingly good when we consider that many of the rules of GTD were violated as far as the distance to diffracting edges is concerned. The goal of obtaining radiation patterns within 3dB to 6 dB for the initial ship design phases have

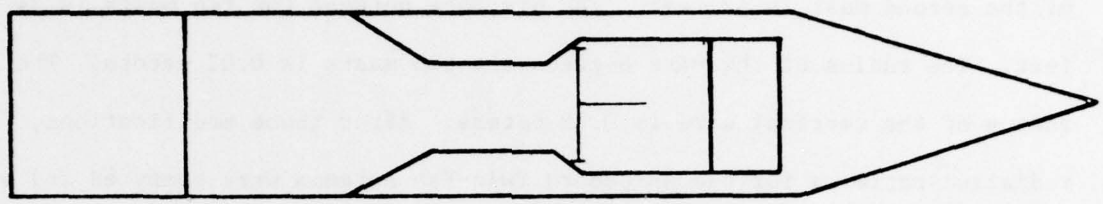

FIG. 21-(a) MODEL FOR SHIP AND TWIN-FAN ANTENNA

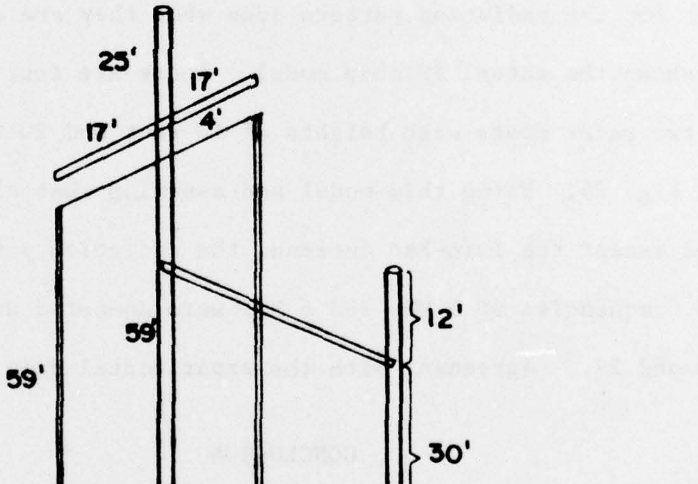

FIG. 21-(b) MODEL FOR TWIN-FAN ANTENNA

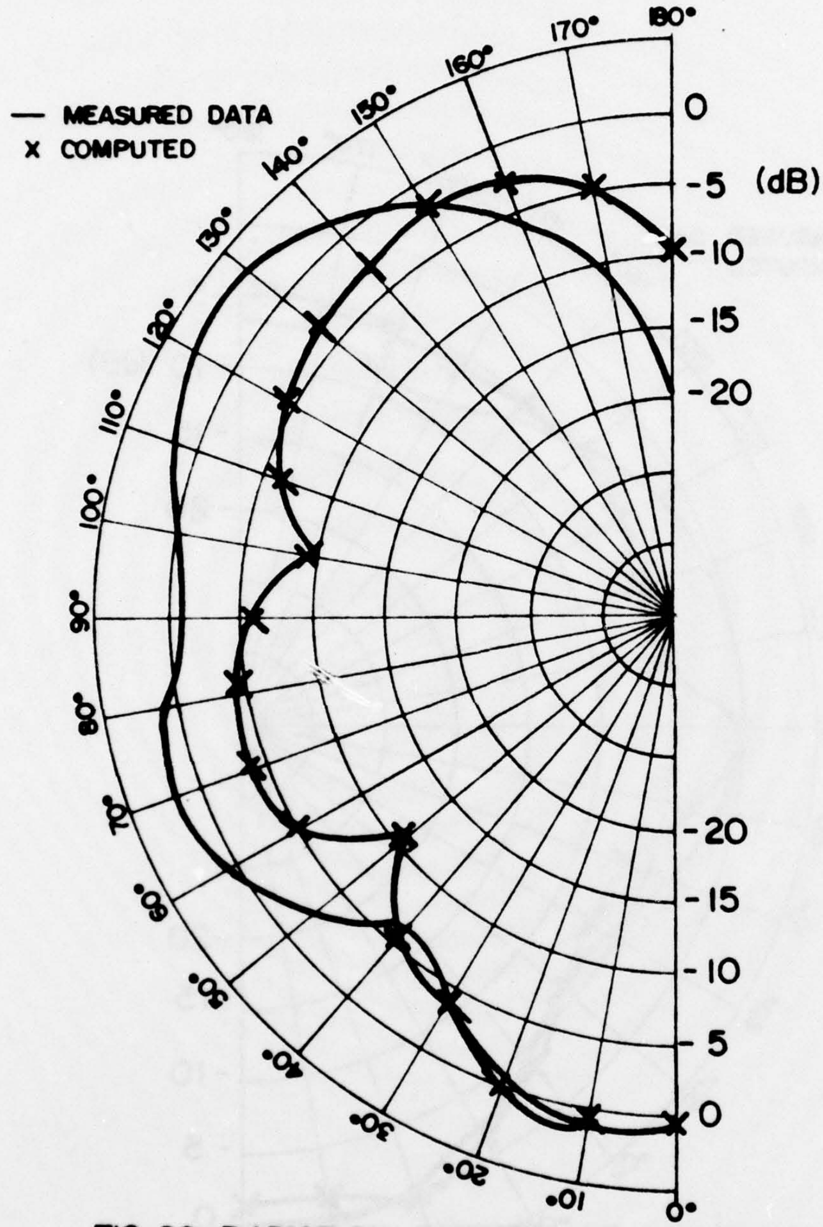

FIG. 22 RADIATION PATTERN OF SHIPBOARD TWIN-FAN ANTENNA FOR THE MODEL OF FIG. 21 AT 10° ELEVATION AND f = 6 MHz (VERTICAL POLARIZATION)

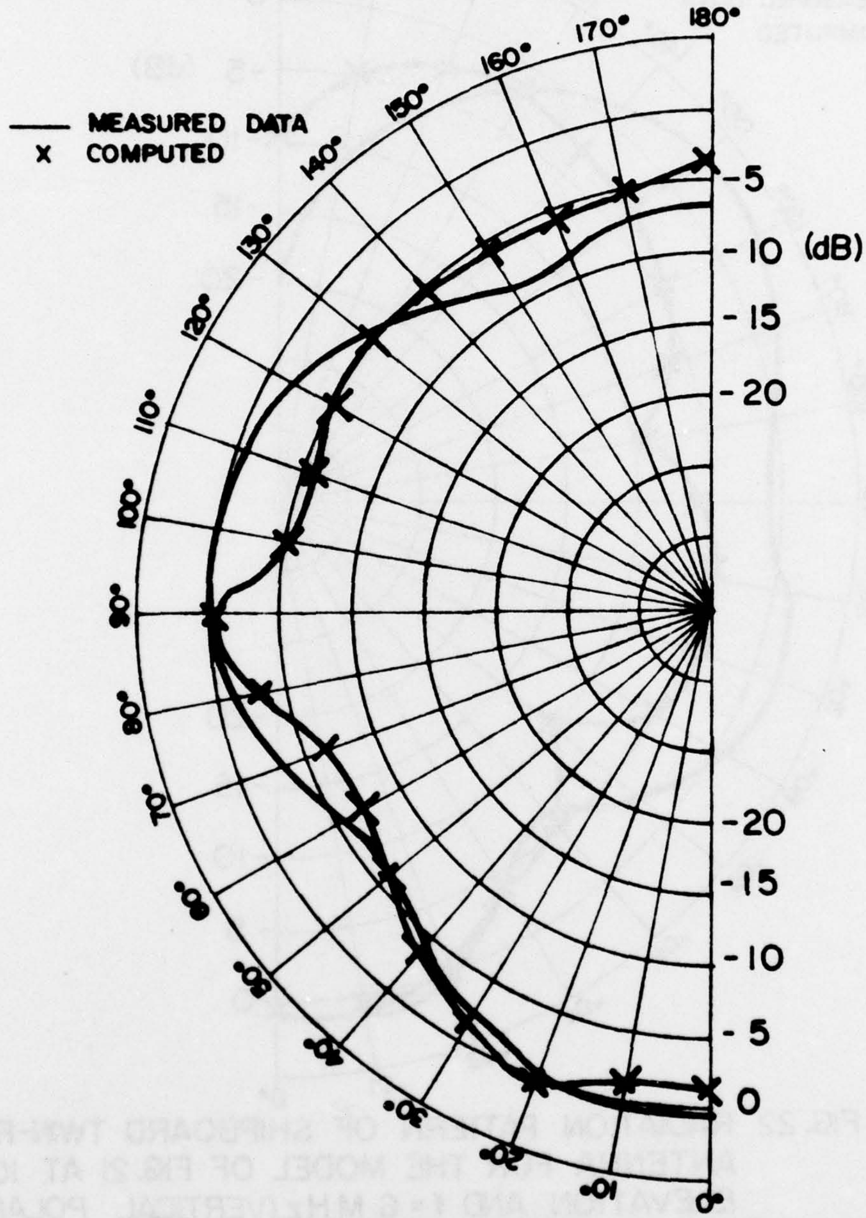

FIG. 23 RADIATION PATTERN OF SHIPBOARD TWIN-FAN ANTENNA FOR THE MODEL OF FIG. 21 AT 10° ELEVATION AND f = 5 MHz (VERTICAL POLARIZATION)

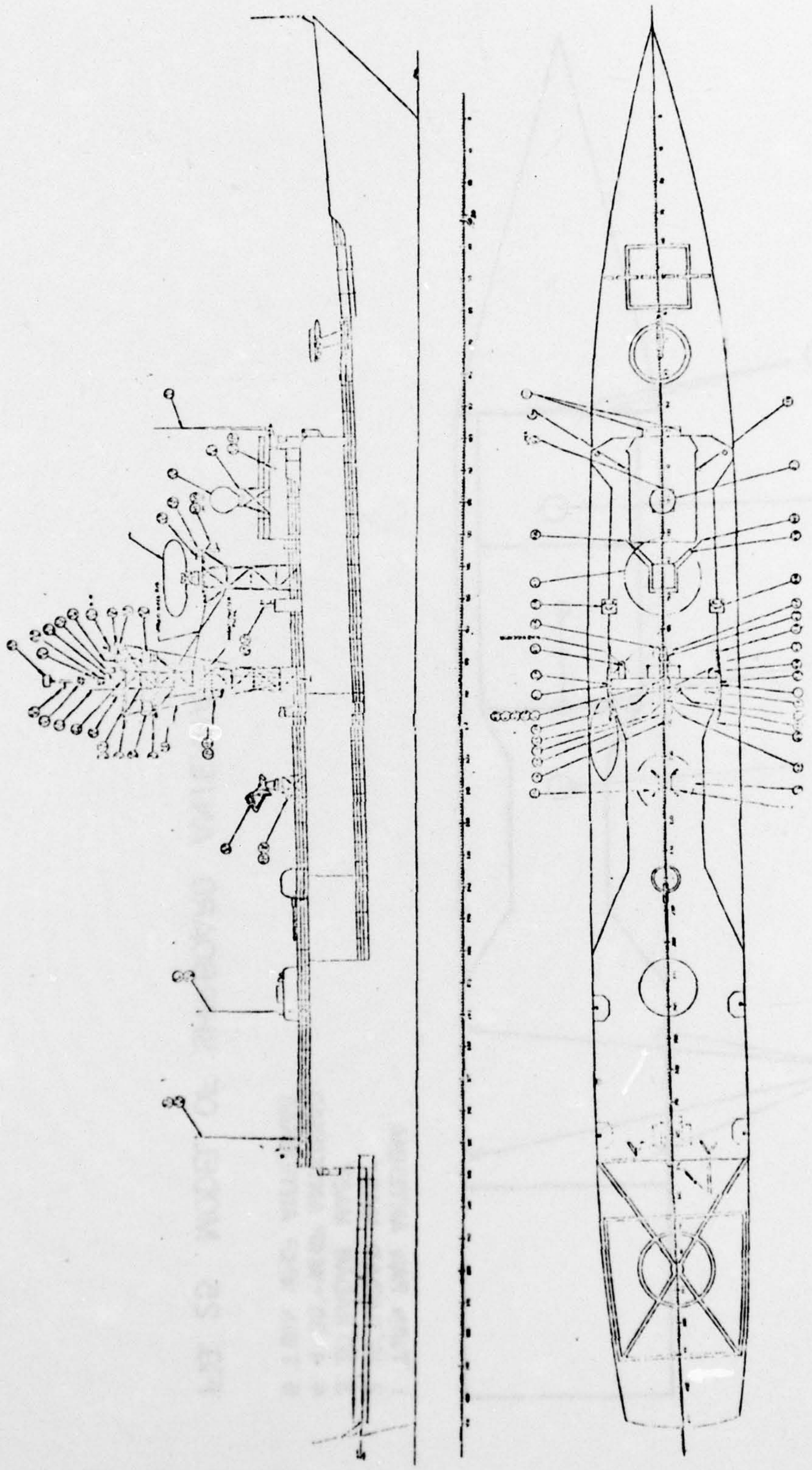

Fig. 24. Patrol Frigate.

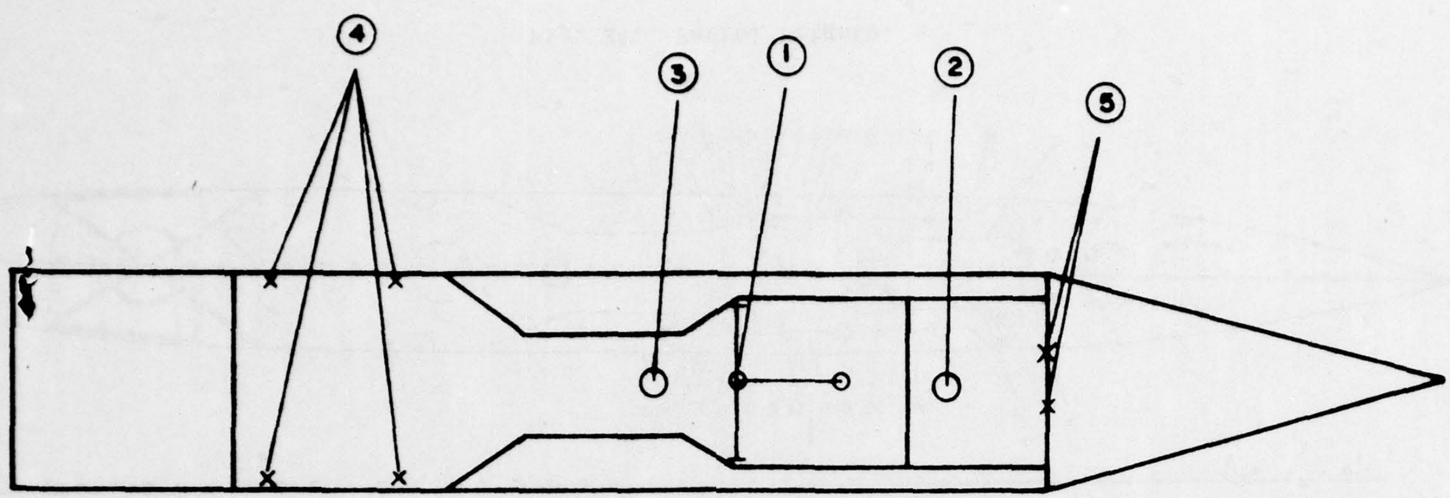

1 TWIN FAN ANTENNA
2 18' RADAR MAST
3 20' RADAR MAST
4 4 35'-WHIP ANTENNAS
5 TWIN WHIP ANTENNAS

FIG. 25 MODEL OF SHIPBOARD ANTENNA

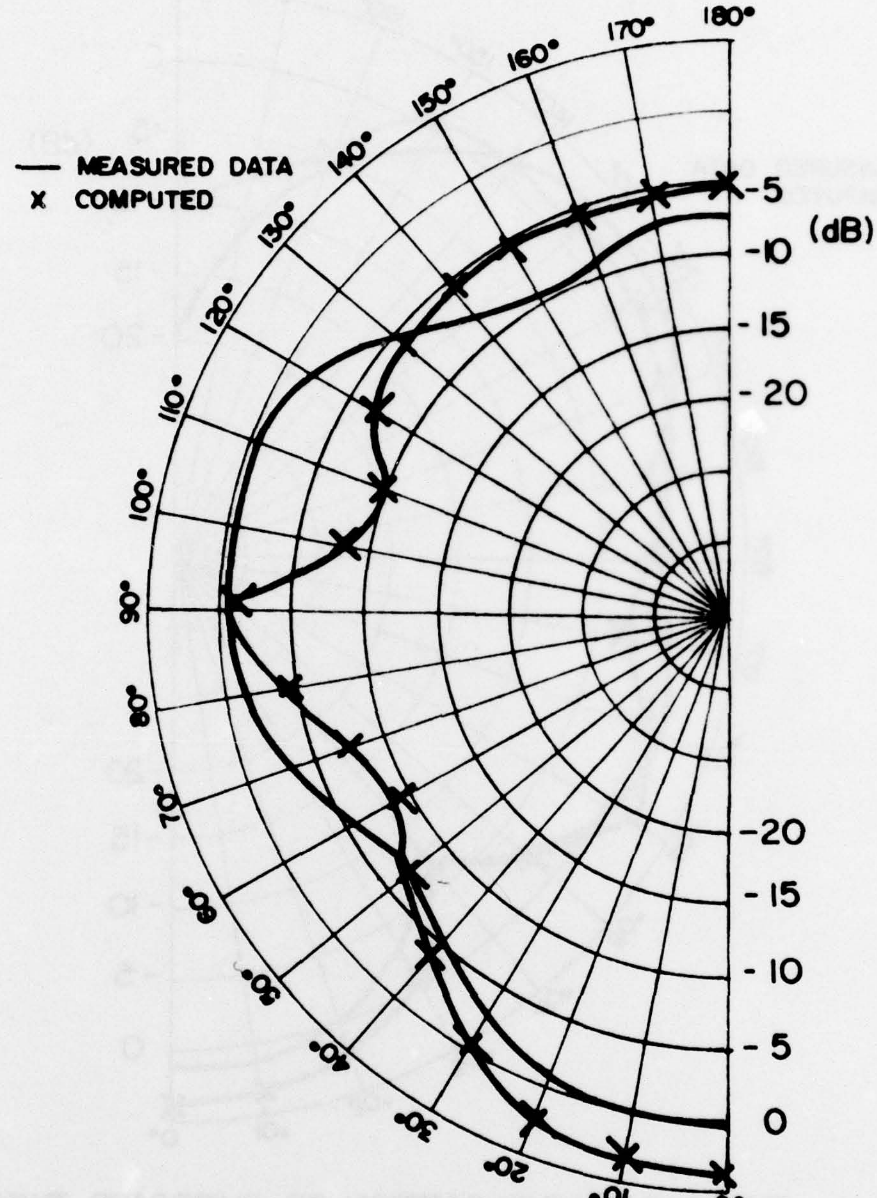

FIG. 26 RADIATION PATTERN OF SHIPBOARD TWIN-FAN ANTENNA FOR MODEL OF FIG. 25 WITH ALL ANTENNAS OPEN-CKTED EXCEPT TWIN-FAN ANTENNA AT 10° ELEVATION AND f=5 MHz (VERTICAL POLARIZATION)

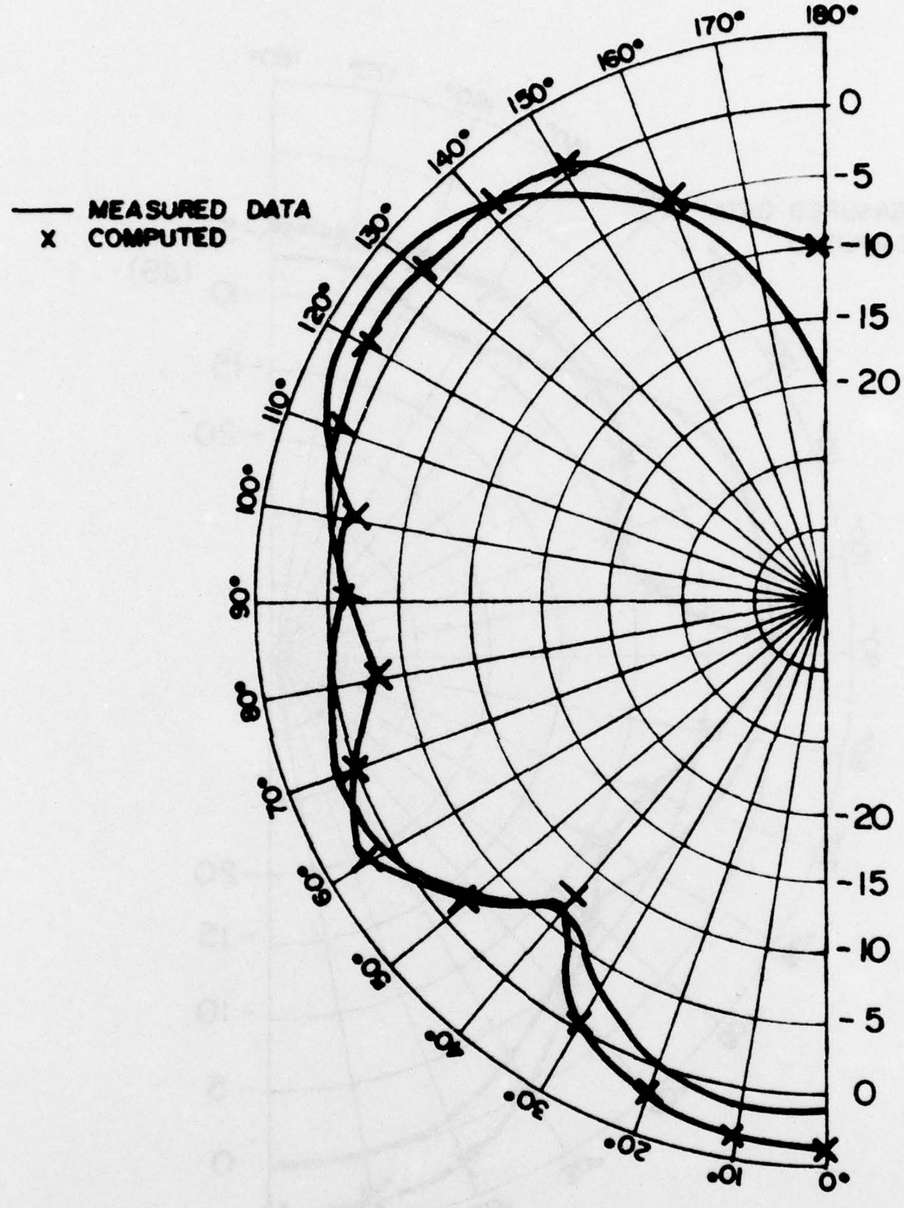

FIG. 27 RADIATION PATTERN OF SHIPBOARD TWIN-FAN ANTENNA FOR MODEL OF FIG. 25 WITH ALL ANTENNAS OPEN-CKTED EXCEPT TWIN-FAN ANTENNA AT 10° ELEVATION AND f = 6 MHz (VERTICAL POLARIZATION)

generally been met.

We feel that we have to gain more experience in applying this technique to ship design to decide what can be neglected and what should be considered in the computational mode. This should be the main thrust of a follow up effort.

REFERENCES

[1] R. F. Harrington, Field Computation by Moment Methods, MacMillan, New York, 1968.

[2] J. R. Mautz and R. F. Harrington, "Radiation and Scattering From Bodies of Revolution", Appl. Sci. Res., June 1969, vol. 20, pp. 425-435.

[3] G.A. Thiele, T.H. Newhouse,"A Hybrid Technique for Combining Moment Methods with the Geometrical Theory of Diffraction", IEEE AP-23, Jan.1975,62-69.

[4] W. P. Burnside, "Analysis of On-Aircraft Antenna Patterns", Technical Report, Ohio State University, Aug. 1972, pp. 3370-3371.

[5] R. G. Kouyoumjian and P. H. Pathak, "The Dyadic Diffraction Coefficient for a Curved Edge", Report 3001-1, Electro Science Lab., The Ohio State University, 1973.

[6] P. H. Pathak and R. G. Kouyoumjian, "The Dyadic Diffractions Coeffi- for a Perfectly-Conducting Wedge", Report 2183-4, Electro Science Lab., The Ohio State University, 1970.

[7] R. G. Kouyoumjian and P. H. Pathak, "A Uniform Geometrical Theory of Diffraction for an Edge in a Perfectly Conducting Surface," Proc. IEEE, vol. 62, No. 11, Nov. 1974, pp. 1448-1461.

[8] C. E. Ryan, Jr., and L. Peters, Jr., "A Creeping Wave Analysis of the Edge on Echo Area of Disk", IEEE, AP-16, No. 2, March 1968, p. 274.

[9] W. D. Burnside, C. L. Yu, and R. J. Marhefka, "A Technique to Combine the Geometrical Theory of Diffraction and the Moment Method", IEEE, AP-23, July 1975, pp. 551-558.

[10] J. S. Yu and R. C. Rudduck, "Diffraction by Conducting Walls of Finite Thickness", Ohio State University, Report 1767-7, May, 1965.

[11] N. Morita, "Diffraction by Arbitrary Cross-Sectional Semi-Infinite Conductor", IEEE, AP-19, May 1971, pps. 358-364.

[12] J. S. Yu, R. C. Rudduck, and L. Peters, Jr., " Comprehensive Analysis for E-plane of Horn Antennas by Edge Diffraction Theory", IEEE, AP-14, March 1966.

[13] C.E. Ryan, Jr. and L. Peters, Jr., "Evaluation of Edge Diffracted Fields Including Equivalent Currents for the Caustic Regions," IEEE, AP-17, May 1969, pp. 292-299.

[14] P.A.J. Ratnasin, R.G. Kouyoumjian and P.H. Pathak, "The Wide-Angle Sidelobes of Reflector Antennas," Ohio State University, Electro Science Lab., Report No. 2183-1, March 1970.

[15] C.E. Ryan, Jr. and R.C. Rudduck, "A Wedge Diffraction Analysis of the Radiation Patterns of Parallel Plate Waveguides," IEEE, AP-16, July 1968, p. 490.

[16] J.B. Keller, "Diffraction by an Aperture," J. of Applied Physics, Vol. 28, April 1957, pp. 426-444.

[17] J.B. Keller, "Geometrical Theory of Diffraction," J. Opti. Soc. Amer, Vol. 52, Feb. 1962, pp. 116-130.

[18] R.R. Raschke, "Computer Calculated Patterns of the PF Twin-Fan Antenna in the Shipboard Environment," Technical Brief, PF No. 2A.

[19] R.I. Goodbody and W.H. Kelly, "Patrol Frigate Radio Communication Antenna System," Technical Document 243, Naval Electronics Lab. Center, San Diego, CA, April 1973.

[20] "Radiation Pattern and Isolation Data from 1:48 Scale PF Ship Model Analysis," Engineering Report, Aug. 1973. SM. No. 73 DECO-2.

METRIC SYSTEM

BASE UNITS:

Quantity	Unit	SI Symbol	Formula
length	metre	m	...
mass	kilogram	kg	...
time	second	s	...
electric current	ampere	A	...
thermodynamic temperature	kelvin	K	...
amount of substance	mole	mol	...
luminous intensity	candela	cd	...

SUPPLEMENTARY UNITS:

Quantity	Unit	SI Symbol	Formula
plane angle	radian	rad	...
solid angle	steradian	sr	...

DERIVED UNITS:

Quantity	Unit	SI Symbol	Formula
Acceleration	metre per second squared	...	m/s
activity (of a radioactive source)	disintegration per second	...	(disintegration)/s
angular acceleration	radian per second squared	...	rad/s
angular velocity	radian per second	...	rad/s
area	square metre	...	m
density	kilogram per cubic metre	...	kg/m
electric capacitance	farad	F	A·s/V
electrical conductance	siemens	S	A/V
electric field strength	volt per metre	...	V/m
electric inductance	henry	H	V·s/A
electric potential difference	volt	V	W/A
electric resistance	ohm		V/A
electromotive force	volt	V	W/A
energy	joule	J	N·m
entropy	joule per kelvin	...	J/K
force	newton	N	kg·m/s
frequency	hertz	Hz	(cycle)/s
illuminance	lux	lx	lm/m
luminance	candela per square metre	...	cd/m
luminous flux	lumen	lm	cd·sr
magnetic field strength	ampere per metre	...	A/m
magnetic flux	weber	Wb	V·s
magnetic flux density	tesla	T	Wb/m
magnetomotive force	ampere	A	...
power	watt	W	J/s
pressure	pascal	Pa	N/m
quantity of electricity	coulomb	C	A·s
quantity of heat	joule	J	N·m
radiant intensity	watt per steradian	...	W/sr
specific heat	joule per kilogram-kelvin	...	J/kg·K
stress	pascal	Pa	N/m
thermal conductivity	watt per metre-kelvin	...	W/m·K
velocity	metre per second	...	m/s
viscosity, dynamic	pascal-second	...	Pa·s
viscosity, kinematic	square metre per second	...	m/s
voltage	volt	V	W/A
volume	cubic metre	...	m
wavenumber	reciprocal metre	...	(wave)/m
work	joule	J	N·m

SI PREFIXES:

Multiplication Factors	Prefix	SI Symbol
1 000 000 000 000 = 10^{12}	tera	T
1 000 000 000 = 10^{9}	giga	G
1 000 000 = 10^{6}	mega	M
1 000 = 10^{3}	kilo	k
100 = 10^{2}	hecto*	h
10 = 10^{1}	deka*	da
0.1 = 10^{-1}	deci*	d
0.01 = 10^{-2}	centi*	c
0.001 = 10^{-3}	milli	m
0.000 001 = 10^{-6}	micro	μ
0.000 000 001 = 10^{-9}	nano	n
0.000 000 000 001 = 10^{-12}	pico	p
0.000 000 000 000 001 = 10^{-15}	femto	f
0.000 000 000 000 000 001 = 10^{-18}	atto	a

* To be avoided where possible.

MISSION
of
Rome Air Development Center

RADC plans and conducts research, exploratory and advanced development programs in command, control, and communications (C^3) activities, and in the C^3 areas of information sciences and intelligence. The principal technical mission areas are communications, electromagnetic guidance and control, surveillance of ground and aerospace objects, intelligence data collection and handling, information system technology, ionospheric propagation, solid state sciences, microwave physics and electronic reliability, maintainability and compatibility.

AMERICAN REVOLUTION BICENTENNIAL 1776-1976